

Original Article

Effect of Buyanghuanwu decoction on hippocampal morphology and expression of LRP1 and ApoJ in APP/PS1 mice

Hongxin Fei^{1,2}, Yusheng Han³, Lili Zhong⁴, Lei Gao⁵, Zhongguang Zhou¹

¹Research Institute of Traditional Chinese Medicine, ³Basic Medical College, ⁴Pathology Department of The First Affiliated Hospital, Heilongjiang University of Chinese Medicine, Harbin 150040, Heilongjiang, China; ²Pathology College, Qiqihar Medical University, Qiqihar, China; ⁵Electron Microscopy Centre, Harbin Medical University, Harbin 150040, Heilongjiang, China

Received December 9, 2016; Accepted November 4, 2017; Epub February 15, 2018; Published February 28, 2018

Abstract: Alzheimer's disease (AD) is the most common degenerative disease of the central nervous system. Buyanghuanwu decoction (BYHWD), a traditional Chinese herbal prescription, has been administrated in APP/PS1 mice with Alzheimer's disease (AD) to detect changes in hippocampal morphology and LRP1 and ApoJ expression. APP/PS1 transgenic mice were classified into 5 groups (n=6), including AD model group, Piracetam treated (0.62 g/kg/d) group, and high-dose (37.06 g/kg/d), medium-dose (18.53 g/kg/d) and low-dose (9.26 g/kg/d) BYHWD treated groups. Meanwhile, wild type (WT) C57BL/6 mice were used as negative controls. Morphological changes were detected by hematoxylin-eosin staining (HE) and transmission electron microscope. LRP1 and ApoJ expressions were measured by using immunohistochemistry assay, quantitative RT-PCR, and western blot assay. Compared with control group, AD model group showed abnormal hippocampus with neuronal loss, capillary stenosis, organelles damage and synaptic alteration, while BYHWD treated groups displayed dose-dependent repair. BYHWD decreases the A β expression in hippocampus of APP/PS1 mice. LRP1 and ApoJ expressions were decreased significantly in AD model compared with WT mice. However, LRP1 and ApoJ expressions significantly increased in high- and medium-dose BYHWD treated groups, compared to AD model group. In conclusion, BYHWD abrogated morphological changes and altered LRP1 and ApoJ expression in hippocampus of AD mice, indicating the neuro-protective role of BYHWD. The mechanism involved maybe through up-regulation of LRP1-mediated pathway.

Keywords: Buyanghuanwu decoction, LRP1, ApoJ, Alzheimer's disease

Introduction

Alzheimer's disease (AD) is the most common cause of dementia and the fourth leading disease in elderly people [1]. According to the neurovascular hypothesis of AD, dysfunctional neurovascular unit could contribute to cognitive impairment by interrupting delivery of nutrients to neurons, and reducing amyloid beta (A β) clearance from the brain [2]. It is conceivable that the damaged neurovascular unit in AD could cause a series of cascade reactions such as neuronal morphological changes and abnormal protein expression, resulting in neurodegeneration [3]. Senile plaques generated by accumulation, aggregation and deposition of A β in brain are widely accepted as the major hallmark of AD [4, 5]. The elevated levels of A β

in brain have been shown to be associated with neuronal and vascular toxicity [6-9], disrupt normal brain function [10] and contribute to cell death [11]. The transport of the A β from brain to blood-brain barrier (BBB) is a major pathway for A β clearance [12, 13]. The rapid elimination of A β efflux is largely mediated by abluminal low density lipoprotein receptor-related protein 1 (LRP1), sequestering some 70% to 90% of plasma A β [12-15]. *In vitro* studies [17, 18] have shown that the soluble A β complexes with LRP ligands, such as apolipoprotein J (ApoJ) [16], apolipoprotein E (ApoE) and α 2-macroglobulin (α 2M) [19], and distinguished by LRP1 and removed out of the brain [20]. However, reduced LRP1 expression at BBB has been found in AD patients [21, 22], making the A β is unfavorable for clearance.

Buyanghuanwu decoction (BYHWD), a traditional Chinese herbal prescription, has been widely employed clinically for improving neurological functional recovery in stroke-induced disability in China for centuries [23]. Recently, extensive researches reported the neuro-protective effect of BYHWD against the ischemic/reperfusion injury [23, 24], found that BYHWD can stimulate neural proliferation and inhibit apoptosis of nerve cells [25]. BYHWD has also been shown to up-regulate vascular endothelial growth factor (VEGF) [26] and angiopoietin-1 (Ang-1) [27] expression in rats after focal cerebral ischemia. Based on these studies, we made an attempt to administer BYHWD in AD mice in order to explore effect of BYHWD on LRP1-related signaling and to determine AD-related targets for its neuro-protective mechanism, which might provide scientific basis for the application of BYHWD in AD.

Materials and methods

Materials

Primary antibodies against LRP1, ApoJ, and β -actin were purchased from Santa Cruz (CA, USA). The PrimeScript RT reagent kit was purchased from TaKaRa Biotechnology (Dalian, China), and the RNeasy Mini kit was obtained from QIAGEN. Piracetam was obtained from Hunan Dinuo Pharmaceutical Co. Ltd (Hunan, China). APP/PS1 (APP^{swe}/PS1^{dE9}) transgenic mice were denoted by Professor Shu-liang Wu from the Department of Anatomy, Harbin Medical University (China). Wild type (WT) C57BL/6 mice were purchased from Beijing Vita River Experimental Animal Technology Co., Ltd (Beijing, China). All the animals were reared at room temperature in the Experimental Animal Center of Heilongjiang University of Chinese Medicine (China).

BYHWD was prepared by Professor Ming Tian from the Experimental Center of Heilongjiang University of Chinese Medicine (China). Radix Astragali, Radix Angelicae Sinensis, Radix Paeoniae Rubra, Rhizoma Chuanxiong, Semen Persicae, Flos Carthami, and Lumbricus were obtained from the First Affiliated Hospital of Heilongjiang University of Chinese Medicine at the ratio of 120:10:10:10:10:10:4.5 (dry weight), respectively, and extracted with water twice. The main effective components of BYHWD

were Astragalus glycosides, ferulic acid, paeoniflorin, safflower yellow pigment, and ligustrazine. The combined filtrate was dried into powder, and stored at 4°C for use.

Model verification

Total RNA extraction for mice hippocampus was performed with Trizol reagent (Life Technologies Corporation) and first strand cDNA was synthesized according to the manufacturer's instructions. Polymerase chain reaction (PCR) was performed in StepOnePlus Real-Time PCR Systems (Applied Biosystems), and analyzed by HMIAS-2000W high-definition color medical image analysis system (Wuhan Champion image technology Co., Ltd). Primer sequences were designed for APP (forward: 5'-GAC TGA CCA CTC GAC CAG GTT CTG-3' and reverse: 5'-CTT GTA AGT TGG ATT CTC ATA TCC G-3'), and PS1 (forward: 5'-AAT AGA GAA CGG CAG GAG CA-3' and reverse: 5'-GCC ATG AGG GCA CTA ATC AT-3') to verify the AD model.

Grouping and administration

Thirty APP/PS1 transgenic mice were divided randomly into five groups (n=6), including APP/PS1 model group, Positive control group (treated with 0.62 g/kg/d Piracetam), and high-dose, medium-dose, and low-dose (37.06 g/kg/d, 18.53 g/kg/d, and 9.26 g/kg/d, respectively) BYHWD treated groups. C57BL/6 mice (WT mice, n=6) that received saline served as negative controls. All mice underwent intragastric administration for 28 d. All animal experiments were approved by the Animal Care and Use Committee, Heilongjiang University of Chinese Medicine, China.

Hematoxylin-eosin (HE) staining

Mice were anesthetized with chloral hydrate 2 h after last administration, filled with 100 ml saline into the left ventricle, and fixed with 4% paraformaldehyde perfusion. Brain tissues were removed and post-fixed in 4% paraformaldehyde and embedded in paraffin. Paraffin sections were treated by dewaxing, dehydration, hematoxylin staining, hydrochloric acid ethanol differentiation, ammonia treatment, eosin staining, ethanol dehydration, transparentization, drying and gum mounting processes before optical microscope observation.

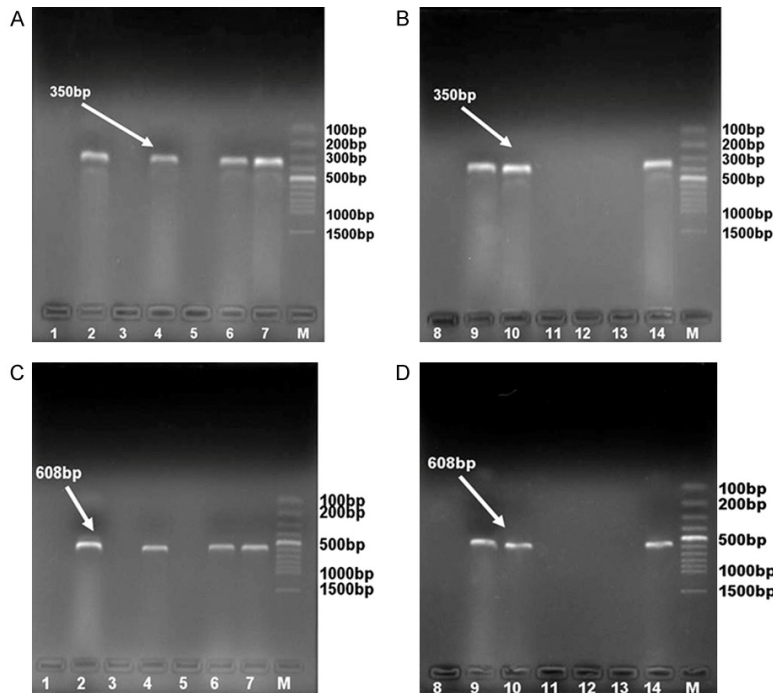


Figure 1. Model verification by agarose gel electrophoresis to detect the expression of APP and PS1 genes after PCR amplification. A, B. Show APP gene, C, D. Show PS1 gene, M represents Marker, band 2, 4, 6, 7, 9, 10, 14 indicate gene from APP/PS1 mice, while band 1, 3, 5, 8, 11, 12, 13 indicate gene from wild type C57BL/6 mice.

Quantitative real-time PCR

Trizol reagent was applied for extraction of total RNA from fresh hippocampal tissues, cDNA reverse transcription and PCR amplification as described above. Primer sequences were synthesized for LRP1 (forward 5'-CCG ACT GGC GAA CAA ATA CAC-3' and reverse 5'-ATC GGC TTT GTT GCA CGT G-3'), ApoJ (forward: 5'-TGA CCC CAT CAC AGT GGT GTT-3' and reverse: 5'-GCT TTT CCT GCG GTA TTC CTG-3'), and β -actin (forward: 5'-CGT GCG TGA CAT CAA AGA GAA-3' and reverse: 5'-AAC CGC TCG TTG CCA ATA GT-3') from Shanghai Generey Biotech Co., Ltd (China). PCR reaction system parameters were as follows: 50°C for 2 min followed by 95°C for 10 min, 95°C for 15 s, 60°C for 1 min, 40 cycles. Amplification

products were analyzed by high-definition color medical image analysis system, and the $\Delta\Delta CT$ method was used to calculate relative expression.

Western blotting

Hippocampus tissue was homogenated with NP-40 lysis buffer (50 mmol/l Tris pH 8.0, 150 mmol/L NaCl, and 1% NP-40) at the proportion of 1 g/ml supplemented with phenylmethane-sulfonyl fluoride (Sigma Aldrich) and PhosSTOP (Roche Diagnostics) at 4°C, and centrifuged at 12,000× g for 10 min. The supernatant was collected as the total protein extract. Protein concentration was estimated using a Pierce BCA Protein Assay Kit (Thermo Scientific) according to the manufacturer's protocol. Equal amounts of protein were analyzed with sodium dodecyl sulfate polyacrylamide gel electrophoresis. Thereafter, proteins were transferred to nitrocellulose membranes and blotted with specific primary antibodies. Proteins were detected via incubation with horseradish peroxidase-conjugated secondary antibodies. Results were analyzed with high-definition color medi-

Transmission electron microscope (TEM)

Hippocampus was isolated and cut into 500 μ m thick transverse slices (Leica CM1900), and fixed by 2.5% glutaraldehyde and OsO₄. After dehydration and embedment in EPON resin, semi-thin sections were stained with 1% toluidine blue and examined using a light microscope. Ultra-thin sections were stained with uranyl acetate and lead citrate was examined by JEM-1200EX (Jeol, Japan).

Immunohistochemistry (IHC)

Paraffin sections were processed by dewaxing, endogenous peroxidase blockade, H₂O₂ treatment, serum blockade before treatment with primary antibody (1:100) at 4°C and biotin-conjugated secondary antibody at 37°C. Then, visualization was done with DAB, followed by dehydration, transparentization and mounting. The number of positive targets were counted by 400× microscope, and analyzed by high-definition color medical image analysis system (HMIAS).

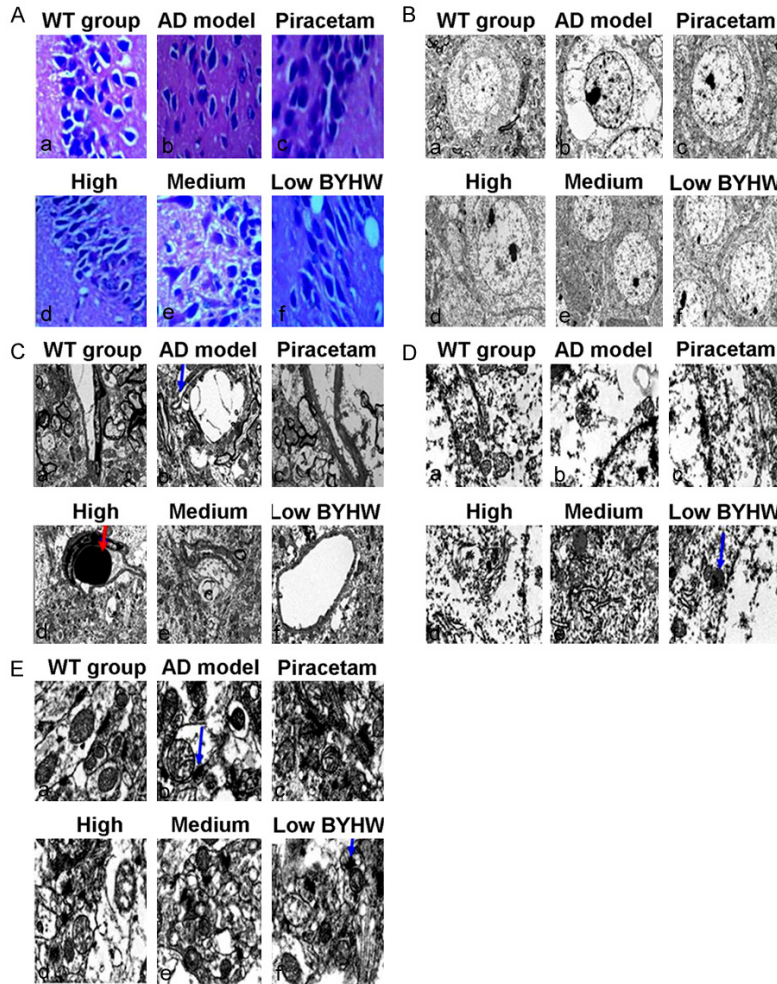


Figure 2. Effect of BYHWD on Hippocampal morphology of APP/PS1 mice. (A) HE staining for the hippocampus (magnification, $\times 400$ in a-f). (a) WT group: neurons were intact and tightly arranged; (b) AD model group: pyramidal neurons presented a densely stained shrunken appearance with minimal cytoplasm. (c) Piracetam-treated group: pyramidal neurons presented a fuzzy staining. (d) High-dose BYHWD treated group: neurons were tightly arranged with regular shape. (e) Medium-dose BYHWD treated group: neurons were scattered with irregular shape. (f) Low-dose BYHWD treated group: Hippocampus presented shrunken pyramidal neurons and obvious vacuoles. (B) Neuronal ultrastructure of the mice hippocampus examined by using TEM (magnification $\times 2550$, a-f). (a) WT group: neurons were arranged regularly with abundant cytoplasm; (b) AD model group: pyramidal neurons had irregular arrangement, condensed organelles and vacuoles. (c-e) Piracetam-treated group, high- and medium-dose BYHWD treated groups: neurons recovered with inerratic array. (f) Low-dose BYHWD treated group: pyramidal neurons had irregular arrangement. (C) Ultrastructure of hippocampal capillary examined by using TEM (magnification, $\times 6000$, a-f). (a) WT group: normal vascular hierarchy with intact endothelium and distinct endothelial cell nucleus; (b) AD model group: capillary wall stenosis with impaired endothelium (blue arrow) and vacuoles. (c) Piracetam-treated group: capillary presented the normal shape as that of WT group. (d and e) High- and medium-dose BYHWD treated groups showed deformed and narrow cerebral arteries, red arrow represents erythrocyte. (f) Low-dose BYHWD treated group displayed obvious vacuoles. (D) Ultrastructure of hippocampal organelles examined by using TEM (magnification, $\times 16500$, a-f). (a) WT group: presented abundant organelles; (b) AD model group displayed few organelles and continuous vacuoles. (c-f) Piracetam-treated group, high-, medium- and low-dose BYHWD treated group: architectures were relatively clear

with increased organelles. Blue arrow represents lipofuscin. (E) Ultrastructure of hippocampal synapses examined by using (magnification, $\times 26500$, a-f). (a) WT group showed greater synapses than (c-e) Piracetam-treated group, and high- and medium-dose BYHWD treated groups; (b) AD model group and (f) low-dose BYHWD treated group displayed severe synaptic elimination (arrows).

cal image analysis system, and the relative contents were displayed by the grey value ratio of indicated protein/ β -actin.

Statistical analysis

Analysis of variance and the post hoc test were used for comparisons across multiple groups. The data is reported as mean \pm standard deviation. Statistical analysis was conducted using SPSS 19.0. $P < 0.05$ was considered statistically significant.

Results

The AD Model was established successfully

After reverse transcription of the total RNA and amplification of the cDNA, both APP and PS1 genes extracted from APP/PS1 transgenic mice were detected simultaneously, while the expression of APP and PS1 genes were not found in WT C57BL/6 mice, verifying the animal models of AD (**Figure 1**).

Morphologic effects of BYHWD on hippocampal morphology in APP/PS1 mice

It has been reported that AD leads to diverse morphological changes in the hippocam-

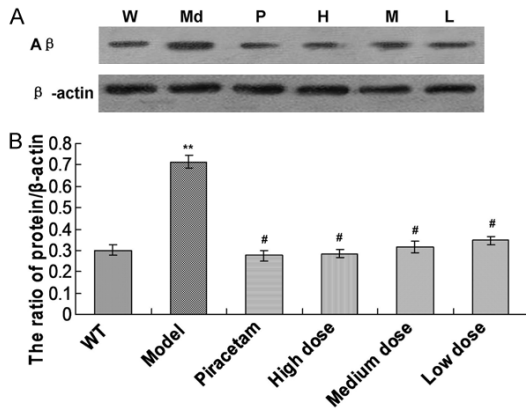


Figure 3. Effect of BYHWD on the A β expression in the hippocampus of APP/PS1 mice. A. A β expression in hippocampal tissues examined by western blot assay. B. Statistical analysis for A β expression in hippocampal tissues. W represents WT group, Md represents model group, P represents Piracetam-treated group, H represents High-dose BYHWD treated group, M represents Medium-dose BYHWD treated group, L represents Low-dose BYHWD treated group.

pus such as neuronal, vascular and synaptic impairment, with resulting neurotransmitter deficits and cognitive symptoms. In the present study, we employed HE staining and TEM to detect the effect of BYHWD on the hippocampus morphology in mice (Figure 2).

Morphologic effects of BYHWD on hippocampal morphology by using HE staining

The hippocampus architecture with HE staining is shown in Figure 2A. In the WT and Piracetam-treated groups, pyramidal neurons were laid in 3-4 layers and arranged tightly with abundant cytoplasm (Figure 2Aa and 2Ac). Remarkable neuronal damage was manifested in the AD model group, which had 2-3 layers of pyramidal neurons and disordered neuronal arrays, accompanied by a large number of glial cell hyperplasia (Figure 2Ab). Progressive neuronal recovery was observed in the BYHWD-treated groups in a dose-dependent manner. High- and medium-dose BYHWD treated group had 3-4 layers of pyramidal neurons with clear structure and even distribution (Figure 2Ad and 2Ae), while the low-dose BYHWD treated group had 2-3 of pyramidal neurons layers with disordered distribution and shallow dying (Figure 2Af), indicating the dose-dependent neuro-protective effect of BYHWD.

Morphologic effects of BYHWD on hippocampal morphology by using TEM examination

At the ultrastructural level, neurons of the WT group had uniform shape, and the nucleus was large and round with abundant cytoplasm (Figure 2Ba). The AD model group hippocampal neurons demonstrated irregular shape, disordered distribution, and condensed organelles (Figure 2Bb). The BYHWD-treated groups gradually regained normal shape with increased dose. Neurons in the BYHWD and Piracetam-treated groups were all regularly shaped (Figure 2Bc-Be). However, low-dose BYHWD treated group displayed shrunk neurons (Figure 2Bf).

We then distinguished the hippocampus capillary at the ultrastructural level. The WT group mice had normal cerebral arteries, intact endothelium and distinct endothelial cell nucleus (Figure 2Ca), while the AD model group had deformed and narrow cerebral arteries, incomplete endothelium, and large vacuoles around the vessel wall (Figure 2Cb). Capillaries of BYHWD- and Piracetam-treated groups were clear and smooth, endothelial cells had no edema, and erythrocytes could be found (Figure 2Cc-Ce). However, the hippocampal capillary shape was compressed with vacuoles in the low-dose BYHWD treated group (Figure 2Cf).

Ultrastructural analysis of the hippocampus showed significant variance in the number of organelles. Hippocampus in the WT group mice was rich in mitochondria and had clear Golgi apparatus (Figure 2Da), while the AD model group mice displayed reduced organelles and increased vacuoles (Figure 2Db). The number of organelles increased in BYHWD and Piracetam-treated groups with relatively obvious architecture (Figure 2Dc-De), and lipofuscin could be seen in the low-dose BYHWD treated group (Figure 2Df).

Synaptic changes were also assessed for BYHWD treatment. Synapses of the WT group were affluent and extended (Figure 2Ea), while the synapses were fused and compressed in the AD model group (Figure 2Eb). The reconstruction of synaptic structure was detected in the high- and medium-dose BYHWD treated and Piracetam-treated groups (Figure 2Ec-Ee). However, no such changes were observed in

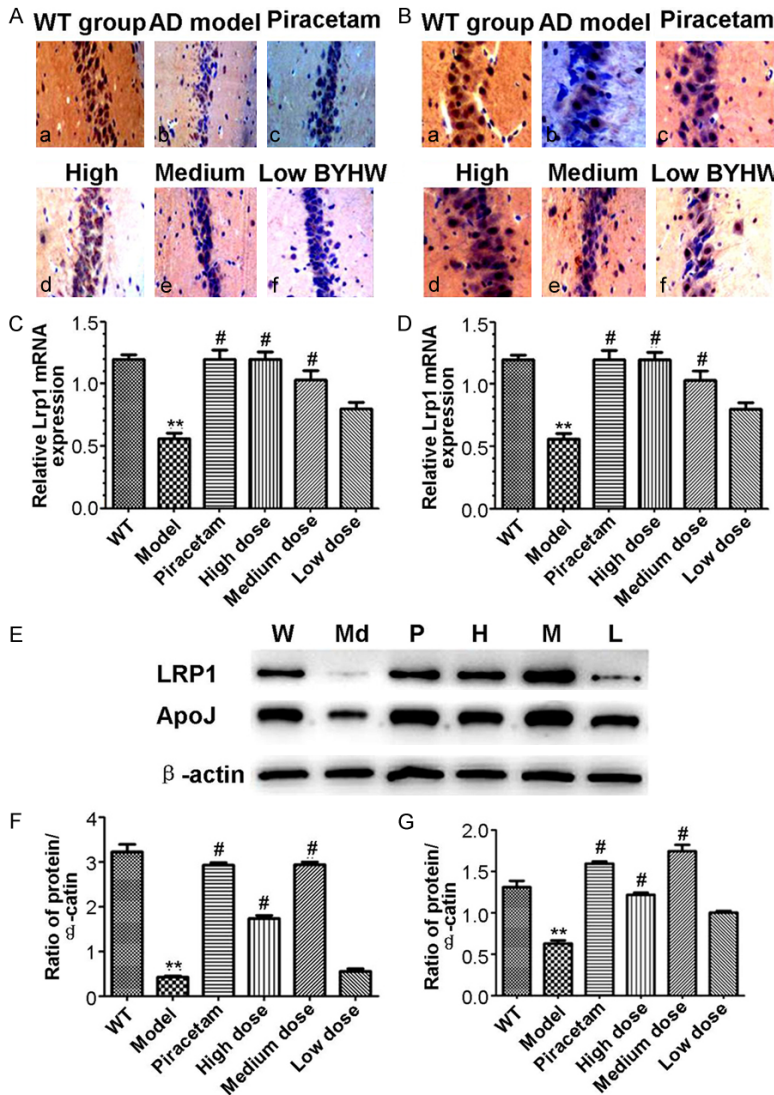


Figure 4. Effect of BYHWD on the expression of LRP1 and ApoJ in the hippocampus of APP/PS1 mice. (A, B) Expression of LRP1 and ApoJ in hippocampal tissues stained by immunohistochemistry assay (magnification, $\times 16500$, a-f). (a) The negative control group (wild type C57BL/6 mice); (b) APP/PS1 model group; (c) The positive control group (treated with Piracetam); (d) High-dose BYHWD treated group; (e) Medium-dose BYHWD treated group; (f) Low-dose BYHWD treated group. (C, D) Relative mRNA expression of LRP1 and ApoJ protein measured by using quantitative RT-PCR. (E-G) Expression of LRP1 and ApoJ protein detected by using western blot assay. W represents WT group, Md represents model group, P represents Piracetam-treated group, H represents High-dose BYHWD treated group, M represents Medium-dose BYHWD treated group, L represents Low-dose BYHWD treated group.

the low-dose BYHWD treated group (Figure 2Ef).

BYHWD decreases the A β expression in the hippocampus of APP/PS1 mice

In order to observe the effects of BYHWD on the A β expression, the A β was examined by

using the western blot assay. The results indicated that the A β levels were significantly increased in AD model group compared to the WT group (Figure 3, $P < 0.05$). Meanwhile, the A β expression was significantly decreased in the BYHWD treatment group compared to the AD model group (Figure 3, $P < 0.05$).

Protective effects of BYHWD on expression of LRP1 and ApoJ in APP/PS1 mice hippocampus

As LRP1 and its related ligands play key roles in the clearance of A β , aggregation of which would cause the pathological event of AD, we determined the effect of BYHWD on the expression of LRP1 and ApoJ in APP/PS1 mice hippocampus by immunohistochemistry, quantitative RT-PCR, and Western blot.

The expressions of LRP1 and ApoJ in the hippocampus were determined by IHC (Figure 4A, 4B). The results showed that both LRP1 and ApoJ expressions in the AD model group were significantly decreased compared with the WT group ($P < 0.05$). After treatment with BYHWD, LRP1 and ApoJ expressions showed a progressive up-regulation with the increasing dose. Compared to the AD model group, LRP1 and ApoJ expressions in the high- and medium-dose BYHWD treated and Piracetam-treated groups increased significantly ($P < 0.05$), while no significant expression level changes were observed in the low-dose BYHWD treated group ($P > 0.05$).

To investigate the mRNA expression levels of LRP1 and ApoJ, we assessed the gene expression levels in the hippocampus of each group.

The results are shown in **Figure 4C, 4D**. The mRNA expression levels of LRP1 and ApoJ in the AD model group decreased significantly, compared to the WT group ($P < 0.05$). After treatment with high- and medium-dose BYHWD and Piracetam, both gene expressions increased significantly compared with the AD model group ($P < 0.05$). Gene expressions in the low-dose BYHWD treated group also increased significantly, compared to the model group, however, the expressions did not reach the normal level ($P < 0.05$).

The LRP1 and ApoJ protein expression levels in the hippocampus were determined by Western blot. The results showed that LRP1 and ApoJ protein expressions were up-regulated by different doses of BYHWD, compared to the AD model group. The expression of LRP1 and ApoJ in the high- and medium-dose BYHWD treated groups restored to the normal levels (**Figure 4E-G**).

Discussion

AD is the most common degenerative disorder of central nervous system, which is characterized by aggregation of A β , resulting in neuronal loss and dysfunction [28]. In the present research, we adopted the APP/PS1 transgenic mice as experimental animals to determine effect of traditional Chinese herbal prescription BYHWD on morphology and the expression of LRP1 and ApoJ in mice hippocampus.

The morphological observation on CA3 area of hippocampus, a part of cortico-hippocampal circuit associated with memory [29], showed typical neuropathological changes in APP/PS1 mice compared with WT mice. HE staining and TEM observations showed distorted cytoarchitecture of neurovascular unit in AD model mice, including neuronal loss, capillary stenosis, organelles damage and synaptic alteration (**Figure 2**). As the neurovascular unit maintains tight control of chemical composition of neuronal internal environment, the neuron loss and capillary stenosis will upset normal neuronal functioning [30]. Cell organelles damage, especially mitochondrial damage, has close connection with neuronal death because of ion homeostasis, such as loss of Na $^+$ /K $^+$ gradient and irregularity of calcium levels [30]. Synaptic alternations in hippocampal tissue and the subsequent release of neurotransmitters has

been suggested to be the major histopathological correlate of cognitive impairment [31].

After being treated with high- and medium-dose BYHWD, the hippocampus almost regained its normal morphology with abundant neurons, clear synapses, increased organelles and regular capillary, thereby, facilitating the constitutive nerve function and metabolism. The low-dose BYHWD treated group displayed poor effect on morphological abnormality of AD model.

Aggregation and deposits of A β have been detected in hippocampus and cortex, which causes the significant damage to neurovascular unit morphology. The A β deposition would create a chronic brain hypoperfusion state, alter the threshold of brain cells to divergent inducers of apoptosis, and enhance the neuronal vulnerability and multiple microinfarctions. LRP1 plays a key role at BBB by facilitating A β transport from brain to blood. Binding of LRP1 to ApoJ could significantly alter A β clearance rates from brain and affect its vascular and parenchymal accumulation [14, 32]. ApoJ, also known as clusterin, acts as an A β chaperone and regulates the conversion of A β to insoluble forms, and influences the transport of A β across the BBB [33, 34]. Binding of ApoJ and A β would increase A β clearance up to 83% in hippocampus [34], indicating the favorable profile of elevated expression of ApoJ for AD treatment.

In the present study, immunohistochemistry, quantitative RT-PCR and western blot assay showed similar results. The expression of LRP1 and ApoJ in hippocampus of AD model group was reduced, demonstrating the attenuated clearance and elevated accumulation of A β . The administration of BYHWD enhanced expression of LRP1 and ApoJ significantly in high- and medium-dose groups. However, no significant increase in expressions of LRP1 and ApoJ were observed in the low-dose BYHWD treated group.

In conclusion, BYHWD abrogated the morphological changes and altered the expression of major transporter LRP1 and its related ligand ApoJ in the AD mice hippocampus, indicating the neuro-protective effect of BYHWD. The underlying mechanism may involve the clearance of A β through up-regulating the LRP1-

mediated pathway. The study will provide a promising strategy in the treatment of AD.

Acknowledgements

The work is funded by the National Natural Science Foundation of China (No. 81373777 and No. 81173599), Heilongjiang Province Qiqihar Science and Technology Bureau of Science and Technology Project (No. SFGG-201630), Heilongjiang Province Qiqihar Medical University Hospital Research Fund Project (No. QY2016B-26).

Disclosure of conflict of interest

None.

Address correspondence to: Zhongguang Zhou, Research Institute of Traditional Chinese Medicine, Heilongjiang University of Chinese Medicine, No. 24, Heping Road, Xiangfang District, Harbin 1500-40, Heilongjiang, China. Tel: +86-451-87266828; E-mail: zhouzhongguang5709@yeah.net

References

[1] Liu CC, Kanekiyo T, Xu H and Bu G. Apolipoprotein E and Alzheimer disease: risk, mechanisms and therapy. *Nat Rev Neurol* 2013; 9: 106-118.

[2] Iadecola C. Neurovascular regulation in the normal brain and in Alzheimer's disease. *Nat Rev Neurosci* 2004; 5: 347-360.

[3] Zlokovic BV. Neurovascular pathways to neurodegeneration in Alzheimer's disease and other disorders. *Nat Rev Neurosci* 2011; 12: 723-738.

[4] Hardy J and Selkoe DJ. The amyloid hypothesis of Alzheimer's disease: progress and problems on the road to therapeutics. *Science* 2002; 297: 353-356.

[5] Blennow K, de Leon MJ and Zetterberg H. Alzheimer's disease. *Lancet* 2006; 368: 387-403.

[6] Hardy J and Selkoe DJ. The amyloid hypothesis of Alzheimer's disease: progress and problems on the road to therapeutics. *Science* 2002; 297: 353-356.

[7] Zlokovic BV, Yamada S, Holtzman D, Ghiso J and Frangione B. Clearance of amyloid beta-peptide from brain: transport or metabolism? *Nat Med* 2000; 6: 718-719.

[8] Paris D, Townsend K and Quadros A. Inhibition of angiogenesis by Abeta peptides. *Angiogenesis* 2004; 7: 75-85.

[9] Tanzi RE, Moir RD and Wagner SL. Clearance of Alzheimer's Abeta peptide: the many roads to perdition. *Neuron* 2004; 43: 605-608.

[10] Haass C and Selkoe DJ. Soluble protein oligomers in neurodegeneration: lessons from the Alzheimer's amyloid beta-peptide. *Nat Rev Mol Cell Biol* 2007; 8: 101-112.

[11] Kim DK, Park JD and Choi BS. Mercury-induced amyloid-beta (Abeta) accumulation in the brain is mediated by disruption of Abeta transport. *J ToxicolSci* 2014; 39: 625-635.

[12] Shibata M, Yamada S, Kumar SR, Calero M, Bading J, Frangione B, Holtzman DM, Miller CA, Strickland DK, Ghiso J and Zlokovic BV. Clearance of Alzheimer's amyloid-ss (1-40) peptide from brain by LDL receptor-related protein-1 at the blood-brain barrier. *J Clin Invest* 2000; 106: 1489-1499.

[13] Deane R, Bell RD, Sagare A and Zlokovic BV. Clearance of amyloid-beta peptide across the blood-brain barrier: implication for therapies in Alzheimer's disease. *CNS Neurol Disord Drug Targets* 2009; 8: 16-30.

[14] Sagare A, Deane R, Bell RD, Johnson B, Hamm K, Pendu R, Marky A, Lenting PJ, Wu Z, Zarcone T, Goate A, Mayo K, Perlmutter D, Coma M, Zhong Z and Zlokovic BV. Clearance of amyloid-beta by circulating lipoprotein receptors. *Nat Med* 2007; 13: 1029-1031.

[15] Zlokovic BV. Neurovascular pathways to neurodegeneration in Alzheimer's disease and other disorders. *Nat Rev Neurosci* 2011; 12: 723-738.

[16] Calero M, Rostagno A, Matsubara E, Zlokovic B, Frangione B and Ghiso J. Apolipoprotein J (clusterin) and Alzheimer's disease. *Microsc Res Tech* 2000; 50: 305-315.

[17] Martel CL, Mackic JB, Matsubara E, Governale S, Miguel C, Miao W, McComb JG, Frangione B, Ghiso J and Zlokovic BV. Isoform-specific effects of apolipoproteins E2, E3, and E4 on cerebral capillary sequestration and blood-brain barrier transport of circulating Alzheimer's amyloid beta. *J Neurochem* 1997; 69: 1995-2004.

[18] Tokuda T, Calero M, Matsubara E, Vidal R, Kumar A, Permann B, Zlokovic B, Smith JD, Ladu MJ, Rostagno A, Frangione B and Ghiso J. Lipidation of apolipoprotein E influences its isoform-specific interaction with Alzheimer's amyloid beta peptides. *Biochem J* 2000; 348 Pt 2: 359-365.

[19] Narita M, Holtzman DM, Schwartz AL and Bu G. Alpha2-macroglobulin complexes with and mediates the endocytosis of beta-amyloid peptide via cell surface low-density lipoprotein receptor-related protein. *J Neurochem* 1997; 69: 1904-1911.

[20] Sousa JC, Cardoso I, Marques F, Saraiva MJ and Palha JA. Transthyretin and Alzheimer's disease: where in the brain? *Neurobiol Aging* 2007; 28: 713-718.

Buyanghuanwu decoction in AD mice

- [21] Bading JR, Yamada S, Mackic JB, Kirkman L, Miller C, Calero M, Ghiso J, Frangione B and Zlokovic BV. Brain clearance of Alzheimer's amyloid-beta40 in the squirrel monkey: a SPECT study in a primate model of cerebral amyloid angiopathy. *J Drug Target* 2002; 10: 359-368.
- [22] Donahue JE, Flaherty SL, Johanson CE, Duncan JA, Silverberg GD, Miller MC, Tavares R, Yang W, Wu Q, Sabo E, Hovanesian V and Stopa EG. RAGE, LRP-1, and amyloid-beta protein in Alzheimer's disease. *Acta Neuropathol* 2006; 112: 405-415.
- [23] Wang L, Huang Y, Wu J, Lv G, Zhou L and Jia J. Effect of Buyanghuanwu decoction on amino acid content in cerebrospinal fluid of rats during ischemic/reperfusion injury. *J Pharm Biomed Anal* 2013; 86: 143-150.
- [24] Li XM, Bai XC, Qin LN, Huang H, Xiao ZJ and Gao TM. Neuroprotective effects of Buyanghuanwu decoction on neuronal injury in hippocampus after transient forebrain ischemia in rats. *Neurosci Lett* 2003; 346: 29-32.
- [25] Wang L and Jiang DM. Neuroprotective effect of Buyanghuanwu decoction on spinal ischemia/reperfusion injury in rats. *J Ethnopharmacol* 2009; 124: 219-223.
- [26] Cai G, Liu B, Liu W, Tan X, Rong J, Chen X, Tong L and Shen J. Buyanghuanwu decoction can improve recovery of neurological function, reduce infarction volume, stimulate neural proliferation and modulate VEGF and Flk1 expressions in transient focal cerebral ischaemic rat brains. *J Ethnopharmacol* 2007; 113: 292-299.
- [27] Shen J, Zhu Y, Yu H, Fan ZX, Xiao F, Wu P, Zhang QH, Xiong XX, Pan JW and Zhan RY. Buyanghuanwu decoction increases angiotensin-1 expression and promotes angiogenesis and functional outcome after focal cerebral ischemia. *J Zhejiang Univ Sci B* 2014; 15: 272-280.
- [28] Butterfield DA, Howard B, Yatin S, Koppal T, Drake J, Hensley K, Aksenov M, Aksenova M, Subramaniam R, Varadarajan S, Harris-White ME, Pedigo NW and Camey JM. Elevated oxidative stress in models of normal brain aging and Alzheimer's disease. *Life Sci* 1999; 65: 1883-1892.
- [29] Kesner RP. Behavioral functions of the CA3 subregion of the hippocampus. *Learn Mem* 2007; 14: 771-781.
- [30] Zlokovic BV. Neurovascular mechanisms of Alzheimer's neurodegeneration. *Trends Neurosci* 2005; 28: 202-208.
- [31] Sigrist SJ and Schmitz D. Structural and functional plasticity of the cytoplasmic active zone. *Curr Opin Neurobiol* 2011; 21: 144-150.
- [32] Deane R, Wu Z, Sagare A, Davis J, Du Yan S, Hamm K, Xu F, Parisi M, LaRue B, Spijkers P, Guo H, Song X, Lenting PJ, Van Nostrand WE and Zlokovic BV. LRP/amyloid beta-peptide interaction mediates differential brain efflux of Abeta isoforms. *Neuron* 2004; 43: 333-344.
- [33] Zlokovic BV, Martel CL, Matsubara E, McComb JG, Zheng G, McCluskey RT, Frangione B and Ghiso J. Glycoprotein 330/megalin: probable role in receptor-mediated transport of apolipoprotein J alone and in a complex with Alzheimer disease amyloid beta at the blood-brain and blood-cerebrospinal fluid barriers. *Proc Natl Acad Sci U S A* 1996; 93: 4229-4234.
- [34] Bell RD, Sagare AP, Friedman AE, Bedi GS, Holtzman DM, Deane R and Zlokovic BV. Transport pathways for clearance of human Alzheimer's amyloid beta-peptide and apolipoproteins E and J in the mouse central nervous system. *J Cereb Blood Flow Metab* 2007; 27: 909-918.